Structure description:

I am studying the vibrational behaviour of a microbeam made of a polymer (Fig. 1(a)) The beam consists of a paddle part and a tapered part and is fixed at the tapered end. The beam material has a double-layered perforation fine structure (Fig. 1(b)). The perforation rate is different on the two layers, which are connected via arrays of pillars. Both perforation and pillars are closer packed in y-direction (the beam length direction) than the x-direction (the beam width direction) to render an anisotropic in plane material property. Fig. 1 (3) shows a unit cell of such a periodic perforation.

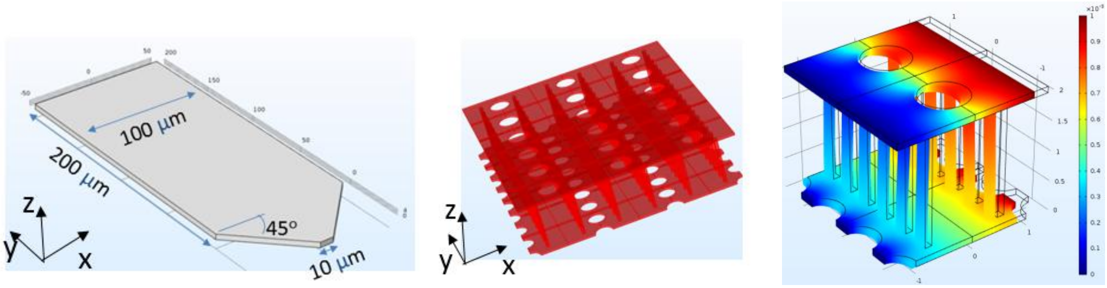

(a) (b) (c)

Fig. 1, (a) a homogeneous microbeam model. (b) the double-layered perforation fine structure of the microbeam. (c) the unite cell of the double-layered perforation.

Key feature sizes of the structure:

Top layer perforation period along x-direction=1.35 um; bottom layer perforation period along x-direction=0.9 um; perforation period along y-direction (both top and bottom layer perforation) =1.3 um; Vertical pillar height= 2 um; top layer and bottom layer thickness=0.1 um

We have already characterized the vibrational spectra of such a microbeam (up to 200 kHz). A numerical model is needed to explain the resonances we observed on the vibrational spectra. Our plan is to first extract the effective material property based on the unit cell of the double-layered perforation (Fig. 1 (c)), and then assigning the material property to the homogeneous microbeam model in Fig. 1 (a) and doing modal analysis in COMSOL.

Problems:

1, The symmetry and tensor form of the double-layered perforation.

The effective material property of a single layer perforation is well established [1]. Its orthotropic symmetry has rendered the effective compliance matrix to have the form in Fig. 2 (c). Paper [1] suggested a whole set of boundary settings to retrieve the effective compliance tensor. These settings rendered the unit cell to experienced either a single pure uni-axial (Fig. 2(a)) or a single shear stress (Fig. 2(b)). The effective strains were then calculated based on the deformation of the unit cell. The corresponding effective compliance components were then calculated.

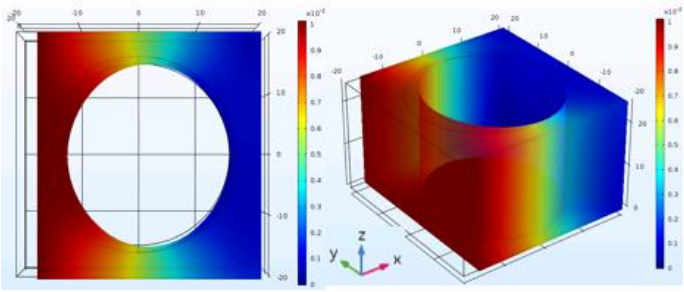

(a)

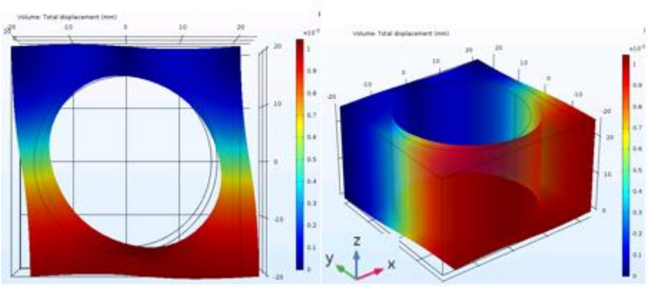

(b)

$$\begin{bmatrix}\varepsilon_{xx}\\ \varepsilon_{yy}\\ \varepsilon_{zz}\\ \gamma_{xy}\\ \gamma_{yz}\\ \gamma_{xz}\end{bmatrix}=\begin{bmatrix}s_{11} & s_{12} & s_{13} & & & \\ s_{12} & s_{22} & s_{23} & & \mathbf{0} & \\ s_{13} & s_{23} & s_{33} & & & \\ & & & s_{44} & 0 & 0\\ & \mathbf{0} & & 0 & s_{55} & 0\\ & & & 0 & 0 & s_{66}\end{bmatrix}\begin{bmatrix}\sigma_{xx}\\ \sigma_{yy}\\ \sigma_{zz}\\ \tau_{xy}\\ \tau_{yz}\\ \tau_{xz}\end{bmatrix}$$

$[\boldsymbol{\sigma}]$=stress tensor

$[\boldsymbol{\varepsilon}]$=strain tensor

$[\boldsymbol{s}]$=compliance tensor

(c)

Fig. 2, model to retrieve the effective elastic compliance of the single layer perforation. The unit cell experiences (a) an uni-axial x-stress; (b) a xy plane shear stress. (c) effective compliance matrix for the single layer perforation.

Although different from the symmetry of the single perforation (point group mmm), double-layered perforation (point group 2mm) also belongs to the orthohombic class. By following the same boundary setting in [1], however, the simulation results got some problem. For example, after introducing the xy shear strain in Fig. 2 (b), paper [1] calculated the effective shear stress of the equivalent unit block by integrating the numerical stress on the top and bottom surfaces of the unit cell in Fig. 2 and divided the integration by the areas of equivalent unit block top and bottom areas (perforation filled). The effective stress obtained this way is the same no matter you calculate it on the top surface or on the bottom surface. Integrating the stress components on the other surfaces show that those effective stress levels are negligible small, so the unit cell essentially gets only one pure shear stress component. For the double-layered perforation, however, by following the same boundary setting, the effective stress calculated on the top surface and on the bottom surface are different. The effective stress levels integrated on the other unit cell surfaces got values comparable with the shear stress level. The same boundary setting failed to introduce a pure shear stress in the double-layered perforation unit cell.

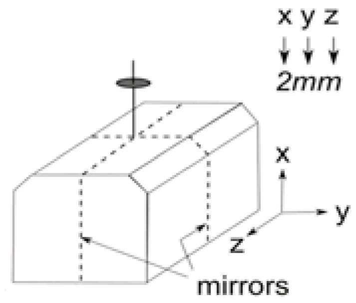

Class	Non-centrosymmetric	Centrosymmetric
Cubic	$23, 432, \bar{4}3m$	$m3, m3m$
Hexagonal	$6, \bar{6}, 622, 6mm, \bar{6}m2$	$6/m, 6/mmm$
Trigonal	$3, 32, 3m$	$\bar{3}, \bar{3}m$
Tetragonal	$4, \bar{4}, 422, 4mm, \bar{4}2m$	$4/m, 4/mmm$
Orthorhombic	$222, 2mm$	mmm
Monoclinic	$2, m$	$2/m$
Triclinic	1	$\bar{1}$

Fig. 3, a crystal processing 2mm symmetry. Table 1, crystal classes and point groups.

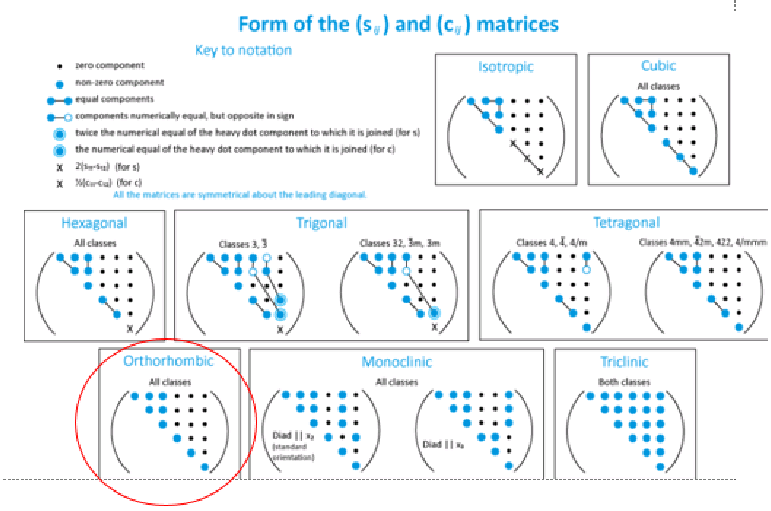

Fig. 4, relation between symmetry and the elastic matrix form.

Questions:

Question 1, Can the double-layered perforation be equivalented to be a homogeneous anisotropic material with the compliance matrix in Fig. 2 (c)? Is the fact that the perforation gets only one period in the thickness direction makes the effective elastic tensor form different? What will be the form?

Question 2, Why the boundary setting which can successfully introduce a pure shear stress in single layer perforation failed when applied to the double-layered perforation?
My understanding is that do not like the single layer perforation, the double-layered perforation top surface and bottom surface are not coincided, when we stack the double-layered perforation unit cell in the z-direction the neighboring surfaces only partially touched. The same boundary setting for single layer perforation is overconstrained for the double-layered perforation.

Question 3, Paper [2] reports a corrugated panel (2mm symmetry) and retrieved its effective plate property. The paper treated the corrugated panel as an orthotropic Kirchhoff plate. Can we also treat the double-layered perforation as a Kirchhoff plate and use the same flexibility matrix (Fig.6) to represent its mechanical property? The micro-beam has the width of 100 micrometre in its paddle part. The thickness/side length ratio in the paddle part is 1/25. The paddle part is thus valid to be treated as a Kirchhoff plate. The width of the beam gradually tapered to 10 micrometer at its clamped end. Will this tapering makes the structure invalid to be treated as a Kirchhoff plate? Is there other effective plate model better suited for this microbeam?

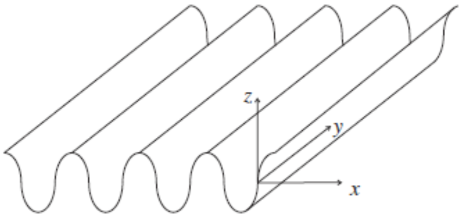

Fig. 5, schematic of a corrugated panel. sheet

$$\mathbf{S} = \mathbf{K}^{-1} = \begin{bmatrix} S_{11} & S_{12} & 0 & 0 & 0 & 0 \\ S_{12} & S_{22} & 0 & 0 & 0 & 0 \\ 0 & 0 & S_{33} & 0 & 0 & 0 \\ 0 & 0 & 0 & S_{44} & S_{45} & 0 \\ 0 & 0 & 0 & S_{45} & S_{55} & 0 \\ 0 & 0 & 0 & 0 & 0 & S_{66} \end{bmatrix}$$

Fig. 6, flexibility matrix of the corrugated composite

Question 4: The fabricated micro-beam in fact got curvature due to processing residue stress. Can the effective plate flexibility tensor be assigned to a curved shell? Will a shell model with the correct curvature (obtained from 3D image of the fabricated microbeam) together with the effective Kirshhoff plate flexibility tensor be enough to predict the vibrational behavior of the microbeam?

Reference:

[1] D. C. Webb, K. Kormi, and S. T. S. Al-Hassani, Use of FEM in performance assessment of perforated plates subject to general loading conditions, Int. J. Pres. Ves. & Piling, vol. 64, 1995, pp. 137-152.

[2] Y. Xia, M.I. Friswell, E.I. Saavedra Flores, Equivalent models of corrugated panels, International Journal of Solids and Structures, vol. 49, 2012.